Mon. Not. R. Astron. Soc. **000**, **??**–**??** (2012) Printed 27 July 2012 (MN LATEX style file v2.2)

Extending gravitational wave burst searches with pulsar timing arrays

Matthew Pitkin[1⋆]
[1]*SUPA, School of Physics and Astronomy, University of Glasgow, University Avenue, Glasgow, G12 8QQ, UK*

ABSTRACT

Pulsar timing arrays (PTAs) are being used to search for very low frequency gravitational waves. A gravitational wave signal appears in pulsar timing residuals through two components: one independent of and one dependent on the pulsar's distance, called the 'Earth term' (*ET*) and 'pulsar term' (*PT*), respectively. The signal of a burst (or transient) gravitational wave source in pulsars' residuals will in general have the Earth and pulsar terms separated by times of the order of the time of flight from the pulsar to the Earth. Therefore, both terms are not observable over a realistic observation span, but the *ET*s observed in many pulsars should be correlated. We show that pairs (or more) of pulsars can be aligned in such a way that the *PT*s caused by a source at certain sky locations can arrive at Earth within a time window short enough to be captured during a realistic observation span. We find that for the pulsars within the International Pulsar Timing Array (IPTA) ~ 67 per cent of the sky produces such alignments for pulsars terms separated by less than 10 years. We compare estimates of the source event rate that would be required to observe one signal in the IPTA if searching for the correlated *ET*s, or in searching via the *PT*s, and find that event rates would need to be about two orders of magnitude higher to observe an event with the *PT*s than the *ET*s. We also find that an array of hundreds of thousands of pulsars would be required to achieve similar numbers of observable events in *PT* or *ET* searches. This disfavours *PT*s being used for all-sky searches, but they could potentially be used target specific sources and be complementary to *ET* only searches.

Key words: gravitational waves, pulsars: general, methods: data analysis

1 INTRODUCTION

In the late 1970s it was first suggested that precision timing of pulsars could be used to detect very low frequency gravitational waves (Sazhin 1978; Detweiler 1979). This lead to early searches for a cosmological stochastic background of nanoHz gravitational waves (e.g. Hellings & Downs 1983; Romani & Taylor 1983; Davis et al. 1985; Rawley et al. 1987; Stinebring et al. 1990; Kaspi, Taylor & Ryba 1994). The first attempt to construct an array of pulsars for use as a gravitational wave detector (amongst other applications) was that of Foster & Backer (1990). More recently several groups around the world (the Parkes Pulsar Timing Array (Verbiest et al. 2010), the European Pulsar Timing Array (Ferdman et al. 2010) and the North American Nanohertz Observatory for Gravitational Waves (Jenet et al. 2009; Demorest et al. 2012)) have worked to set up and perform precision timing of a selection of stable millisecond pulsars. The aim of these is to detect low frequency gravitational waves from objects such as supermassive binary black holes (SBBH). These are now being combined into a concerted world-wide effort to form an International Pulsar Timing Array (IPTA) (Hobbs et al. 2010).

Initial gravitational wave searches using pulsar timing focused on looking for a cosmological stochastic background. Following the theoretical work of Jaffe & Backer (2003) and Wyithe & Loeb (2003) the focus has more recently shifted to finding a stochastic background from multiple SBBHs. Lommen & Backer (2001) performed the first searches for individual quasi-monochromatic SBBH sources (with the more recent theoretical work of Sesana, Vecchio & Volonteri 2009, providing more impetus for this), with this method being used to rule out a putative electromagnetic observation of such a system in the radio galaxy 3C 66B (Jenet et al. 2004). Now there are many proposed methods to detect stochastic sources (e.g. McHugh et al. 1996; Jenet et al. 2005; Anholm et al. 2009; van Haasteren et al. 2009), and several recent searches have been performed providing limits on their emission (e.g. Jenet et al. 2006; Yardley et al. 2011; van Haasteren et al. 2011; Demorest et al. 2012). There are now also many proposed methods to search for individual quasi-monochromatic (or continuous) sources (e.g. Corbin & Cornish 2010; Yardley et al. 2010; Lee et al. 2011; Babak & Sesana 2012; Ellis, Jenet & McLaughlin 2012; Ellis, Siemens & Creighton 2012), and even individual short duration transient (or burst) sources (e.g. van Haasteren & Levin 2010; Pshirkov, Baskaran & Postnov 2010; Finn & Lommen 2010; Cordes & Jenet 2012). A review of the many gravitational wave

⋆ matthew.pitkin@glasgow.ac.uk

search avenues currently being explored can be found in Lommen (2012).

Examples of burst sources could be the final inspiral or parabolic encounters of SBBHs (Finn & Lommen 2010), or cosmic string cusps (Leblond, Shlaer & Siemens 2009; Binétruy et al. 2009; Key & Cornish 2009). Unlike the bursts searched for in ground-based gravitational wave searches (e.g. Abbott et al. 2009), which are generally classed as events lasting of the order of milliseconds–seconds, these *bursts* would last from months to years, but importantly they are transient rather than continuous signals.

1.1 Signals in pulsar timing arrays

Pulsar observers measure the time of arrival (TOA) of pulses, which can be thought of as ticks of a clock. Timing residuals are the difference between the observed TOAs and a best fit model of the time of arrival that is dependent on many parameters such as the pulsar frequency, frequency derivatives, sky position and any binary system parameters if appropriate. Any unmodelled components, such as a potential gravitational wave signal, would remain in the residuals.

A gravitational wave signal appears in pulsar timing residuals through two terms: an 'Earth term' and a 'pulsar term', which we shall refer to as *ET* and *PT* from now on. The *ET* is independent of the pulsar distance and the *PT* is delayed in time from the *ET* by an amount proportional to the pulsar distance. This 'two-pulse' response is more generally the case for any signal in a single-arm one-way gravitational wave detector[1] e.g. Estabrook & Wahlquist (1975) and Detweiler (1979). In this case the pulsar and the receiver on the Earth represent the ends of the arms of the detector. A signal in the *ET* will be simultaneous in all observed pulsar residuals, whereas the *PT* will be delayed by

$$\Delta t = (1 + \hat{\boldsymbol{k}} \cdot \hat{\boldsymbol{n}})d/c, \tag{1}$$

where $\hat{\boldsymbol{k}}$ is a unit vector along the gravitational wave propagation direction (pointing from the source to the Earth), $\hat{\boldsymbol{n}}$ is a unit vector pointing along the Earth-pulsar line-of-sight, and d is the distance to the pulsar. If we define a plane perpendicular to $\hat{\boldsymbol{k}}$ such that the Earth is at the origin and $\hat{\boldsymbol{k}} = \{0, 0, -1\}$, and $\hat{\boldsymbol{n}} = \{\sin\theta\cos\phi, \sin\theta\sin\phi, \cos\theta\}$, where θ is the polar angle between the source and pulsar, and ϕ is the azimuthal angle from some arbitrary point (which for the moment does not matter), then

$$\Delta t = (1 - \cos\theta)d/c. \tag{2}$$

As stated in Finn & Lommen (2010), unless the pulsar and source are closely aligned on the sky, this time delay will be large. So, for a transient burst source if the *ET* is observed then the *PT* will not appear in the residuals over the typical period of pulsar observations of one-to-two decades. For this reason the *PT* is often ignored. The inclusion of the *PT*, and extra information that can be gathered from it (e.g. pulsar distance measurements (Sazhin 1978; Lommen 2001; Jenet et al. 2004; Yardley et al. 2010; Corbin & Cornish 2010; Lee et al. 2011), source distance via parallax (Deng & Finn 2011) or studying a signal at different times in its evolution (Mingarelli et al. 2012)), has been studied with regard to continuous gravitational wave signals, but not for burst sources.

[1] Note that for ground-based gravitational wave detectors, where the wavelength of the gravitational wave is far longer than the arm length, the 'two-pulse' structure and frequency dependence disappear from the detector response (e.g. Finn 2009).

However, pulsar timing arrays (PTAs) consist of many pulsars. This brings the possibility that among pairs, or more, of pulsars there might be fortuitous lines-of-sight where the time delay between *PT*s in particular pulsars is small enough to be within an observational data set. This is the possibility we explore in Section 2 of this paper.

In a standard burst search using just the *ET*s all pulsars in the array can be coherently analysed giving the maximum possible sensitivity, but temporally it is limited to signals that are passing the Earth now (or at least to within the decade or so over which the PTA is observing). Looking for signals in the *PT* will not give as good sensitivity as that from a coherent *ET* search, because only two (or a few) pulsars can be coherently combined, but each pulsar pair will provide a different time baseline in which to search. These signals would otherwise not be observed *at all* in an *ET*-only search. So, given the temporal coverage it provides it could still be a worthwhile area to search. We will explore this more in Section 3.

2 INTER-PULSAR TIME DELAYS

In this section we will consider the 30 pulsars of the IPTA as given in Finn & Lommen (2010). Here we look at the minimum time delay between the *PT*s for all pairs of pulsars in the array for sources located across the sky. For a pulsar i with right ascension and declination α_i and δ_i, distance d_i, and a source position α_s and δ_s, with a distance L emitting at t_0, the time of arrival of the *PT* at the Earth will be

$$t_i = t_0 + L/c + (1 - \cos\theta_i)d_i/c, \tag{3}$$

where the angular separation between the source and pulsar is

$$\theta_i = \arccos\left\{\cos(a)\cos(b) + \sin(a)\sin(b)\cos(|\alpha_i - \alpha_s|)\right\}, \tag{4}$$

with $a = \pi/2 - \delta_i$ and $b = \pi/2 - \delta_s$. So, for a pair of pulsars i and j the difference between the time of arrival of the *PT* for a source at a given sky position is

$$\Delta t_{ij} = |t_i - t_j| = |(1 - \cos\theta_i)d_i - (1 - \cos\theta_j)d_j|/c. \tag{5}$$

A schematic of this set-up for a pair of pulsars is shown in Figure 1. It is important to note that the delay δt in the figure is not the time delay between the *PT*s, because the information that the gravitational wave has influenced the pulsar still has to travel to Earth encoded in the electromagnetic pulses. Thus the real time difference is given by Δt_{21}. Figure 2 shows how the time delay, Δt_{21}, between the times-of-arrival of the *PT*s observed in pulsar residuals at Earth for a PTA consisting of a pair of pulsars (J1455−3330 with $\alpha = 14^{\mathrm{h}}55^{\mathrm{m}}47\overset{\mathrm{s}}{.}9$, $\delta = -33^\circ30'46\overset{''}{.}3$ and distance of 0.74 kpc, and J2129−5721 with $\alpha = 21^{\mathrm{h}}29^{\mathrm{m}}22\overset{\mathrm{s}}{.}7$, $\delta = -57^\circ21'14\overset{''}{.}1$ and a distance of 0.53 kpc) changes for sources located across the whole sky. It can be seen that the minimum in the delay forms a ring on the sky. The overlap of many such rings can be seen later in Figure 4.

If we choose a constraint such that in Equation 5 $\Delta t_{ij} <$ 10 years then Figure 3 shows the valid areas of the θ_i, θ_j, d_i and d_j parameter space that fulfil this criterion. It can be seen that in the extreme cases where one pulsar is closely aligned on the sky with the source, and the other is on the opposite side of the sky to the source (e.g. $\theta_{i,j} \approx 0^\circ$ and $\theta_{j,i} \approx 180^\circ$) then the pulsar distance ratio must be very large to fulfil the criterion.

In this paper we will assume a time delay between *PT*s of less than 10 years is reasonable for searches on current, or near future, sets of data. Using a grid of source sky positions and all

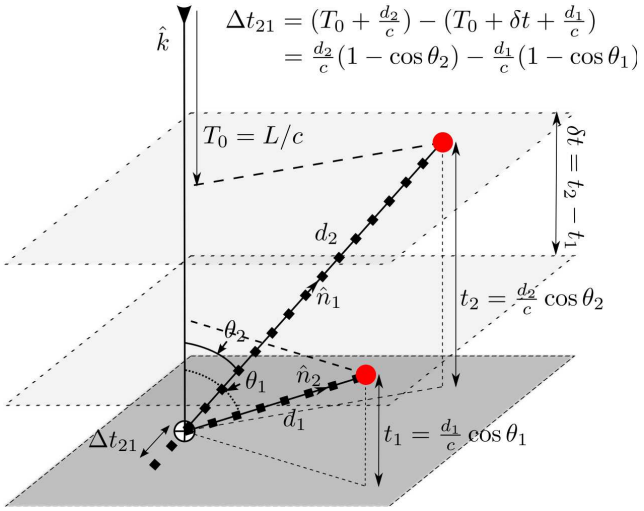

Figure 1. A schematic diagram showing the geometry of two pulsars, a passing plane gravitational wave and the Earth $\oplus$. From top to bottom the planes correspond to the gravitational wave intersecting the first pulsar, then the second pulsar and then the Earth. The time delay between the *PT*s is given as Δt_{21}.

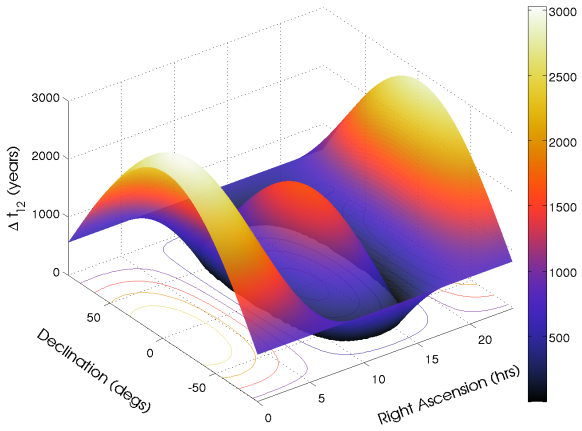

Figure 2. The time delay between the *PT*s from Equation 5 as a function of source sky position for a pulsar pair consisting of J1455−3330 ($\alpha = 14^{\rm h}55^{\rm m}47\overset{\rm s}{.}9$, $\delta = -33^\circ30'46\overset{''}{.}3$ and distance of 0.74 kpc) and J2129−5721 ($\alpha = 21^{\rm h}29^{\rm m}22\overset{\rm s}{.}7$, $\delta = -57^\circ21'14\overset{''}{.}1$ and a distance of 0.53 kpc).

the pulsars in the IPTA, we have calculated the minimum value of Δt_{21} in years for all pulsar pairs, the sky area for which this delay is less than 10 years and the total number of pulsar pairs for which this delay is less than 10 years. These are shown as Hammer projections onto the sky in Figure 4. Obviously for longer spans of data longer time delays can be contemplated and more pulsar pairs will be usable. Figure 4(b) shows the sky area available if we exclude all sky positions for which no *PT* time delay is less than 10 years. This shows that 67 per cent of the sky will contain at least one pair of pulsars with a time delay between *PT*s of less than 10 years. Residuals for any such pair could then be cross correlated with the appropriate delay applied for the sky position.

Figure 4(c) shows the total number of pulsar pairs that would have time delays of less than 10 years for each sky position of the

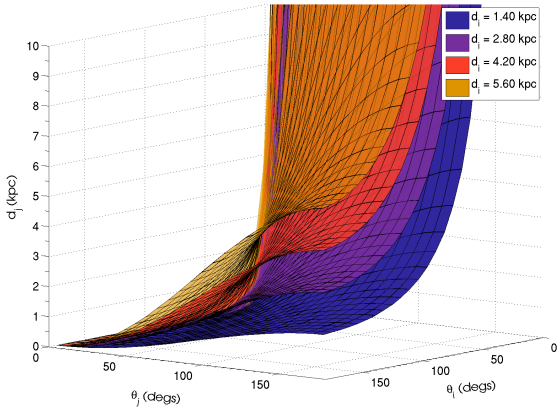

Figure 3. The sheets represent regions in the θ_i, θ_j, d_i and d_j parameter space for a pair of pulsars that fulfil the criterion from Equation 5 that $\Delta t_{ij} < 10$ years.

gravitational wave source. We see that there are some small patches of the sky where up to 11 pulsar pairs are usable. However, it is unlikely that multiple pairs of pulsars would have the same individual signal in them for a given sky position. Unfortunately this means that generally coherent analyses between multiple pairs are not viable, but having multiple pairs gives you a higher effective temporal observation span (as discussed in Section 3). There are sky locations for which more than two IPTA pulsars are aligned as such to fulfil the time delay criterion, but the sky area covered is general small. Figure 5(a) shows that for the IPTA we find 5.6 per cent of the sky for which the *PT* for three pulsars are within 10 years of each other, 0.3 per cent for which there are four pulsars and 0.005 per cent for which there are the maximum of five pulsars.

2.1 Expanding the PTA

In the future when more pulsars are added to an array more sky areas with multiple pulsar overlap (i.e. > 2) may be available, in particular with the addition of many pulsars within the same globular cluster, which are physically separated by short (of order years) delays. An example of how co-located pulsars in globular clusters can be used in gravitational wave detection is given by Jenet, Creighton & Lommen (2005). As a first step at testing how increased numbers of pulsars improve prospects, we have created a fake array by taking all millisecond pulsars currently in the Australian Telescope National Facility (ATNF) pulsar catalogue (Manchester et al. 2005) with frequencies greater than 50 Hz, but not associated with a globular cluster, leaving 90 pulsars. These are just used as an example of what happens when adding more pulsars, however it is not known, or expected, that it will be possible for some, or all, of these specific pulsars to be included in a future array. With this array, and assuming a well-known distance to these pulsars, the source locations for which at least a pair of pulsars has *PT*s within 10 years show over 99.8 per cent sky coverage. We find that the number of pulsars for which the *PT*s are separated by less than 10 years can be up to 8, although this is for one unique sky position ($\alpha = 18^{\rm h}32^{\rm m}23\overset{\rm s}{.}0$ and $\delta = 01^\circ34'44\overset{''}{.}21$) (given a sky pixel of area ~ 0.7 square degrees). The overall number of pulsars with *PT*s within 10 years for all source locations across the sky can be seen in Figure 5(b). In terms of sky area there is 42 per cent of the sky for which 3 pulsars have *PT*s within 10 years, 7 per cent

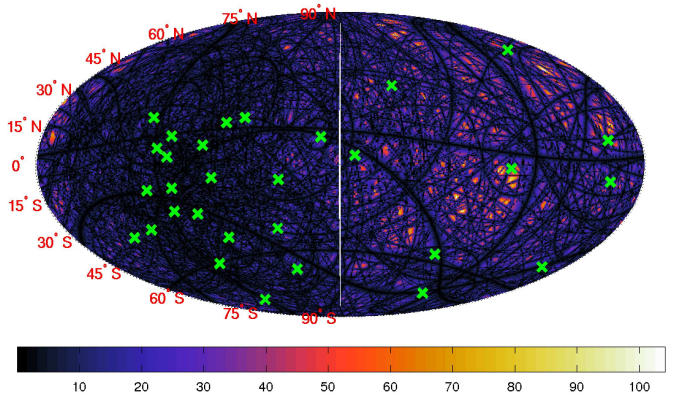

(a)

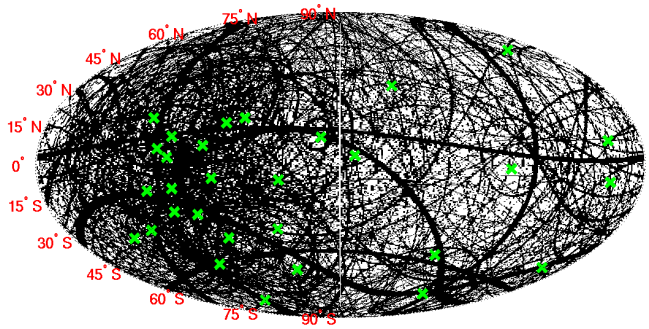

(b)

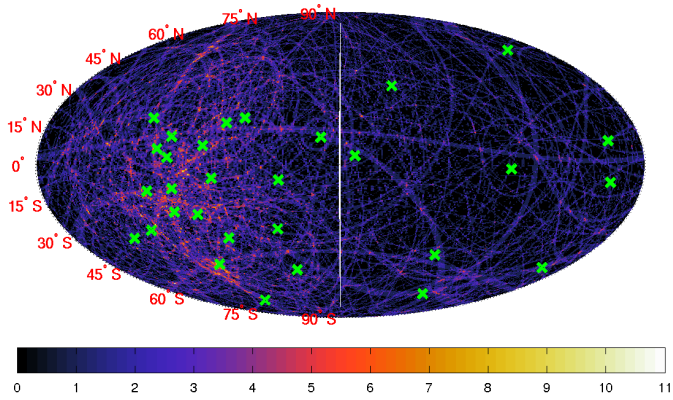

(c)

Figure 4. (a) A Hammer projection sky map giving the minimum time delay between *PT*s over all IPTA pulsar pairs for a source located at each position in the sky. The colour range gives the time delay in years. (b) A map showing only those parts of the sky (black) where a source will produce a signal separated by less than 10 years within at least one pulsar pair. (c) A map showing the number of pulsar pairs for which a source at that sky position would produce a *PT* time delay of less than 10 years. All maps show crosses for the locations of the IPTA pulsars.

with 4 pulsars, ~ 1 per cent with 5 pulsars, ~ 0.08 per cent with 6 pulsars and ~ 0.01 per cent with 7 pulsars. More pulsars in the array can therefore increase the sensitivity for certain sky areas. It should be noted that the sky coverage may be biased by selection effects of observable stable, well-timed, pulsars.

2.2 Distance uncertainties

The initial discussions assume that we know the distances to all the pulsars perfectly, but in reality there will be uncertainties on these distances. Currently these are optimistically of order 10 per cent, but by the time of the Square Kilometre Array (SKA) errors may be reduced to less than 1 per cent for the vast majority of IPTA pulsars, with some of the closest known to maybe a few tenths of a percent (Smits et al. 2011). This uncertainty in the distances means there could be some pulsar pairs that actually lie outside of the required *PT* delay criterion. Conversely, accurate distance estimates could move some pulsar pairs to within the *PT* delay criterion. On average it would be expected that as many pairs move within the criterion as move out of it, but unless the distance uncertainties are included in a search it is not known which move in or out. This means that in reality the area covered in Figure 4(b) would look different, although the total area covered would be approximately the same.

The effect of this means that for a real search the whole sky would have to be covered and the uncertainties in the distances to each pulsar taken into account. So, for each sky position every pulsar pair would have to be tested with the distances of each varied within the uncertainty range.

3 SEARCH COMPARISONS

Many methods have been developed to detect, and estimate parameters, for modelled and unmodelled bursts of gravitational waves in ground-based detectors (e.g. a selection includes Clark et al. 2007; Klimenko et al. 2008; Abbott et al. 2009; Searle, Sutton & Tinto 2009; Sutton et al. 2010), space-based detectors (Babak et al. 2010) and PTAs (e.g. Finn & Lommen 2010; van Haasteren & Levin 2010). It would be relatively straightforward to use similar methods in a search given the situation that we have presented. So, here rather than define another method we will compare aspects of a *PT*-only search with a more standard *ET*-only burst search for a simplified IPTA. The aspects we compare are their sensitivities, their effective observation times, and from these, the estimated event rates required to give a detection.

For this we will compare the signal-to-noise ratio that could be recovered for a single burst source detected in the *ET*s of the IPTA with that which could be recovered for a *PT*-only search. We will make the simplifying assumption that all 30 pulsars within the array have residual noise that is white and Gaussian with standard deviation of 100 ns, all data spans the same 20 years period and they are sampled every 30 days. We will require that to be *detected* a signal must have a signal-to-noise ratio (ρ) above a threshold of 10. We will also assume that all the pulsar distances are precisely known rather than trying to assess the effects searching over some distance uncertainty has on the threshold required for detection[2].

[2] In reality the signal-to-noise ratio threshold at which to set a detection would be lower for the *ET* search than the *PT* search. This is because the background level (e.g. false alarms due to noise) for a signal being observed would be lower due to more detectors being used and the smaller parameter space from not having to search over pulsar distances uncertainties. Therefore, the horizon distance for *ET* searches could be increased by a small factor of the order of 1.25 reducing required rates by a factor of ~ 2.

3.1 The signal model

In these tests we assume a simple signal model of a sine-Gaussian burst. This is defined in the timing residuals of a pulsar (indexed by i) by

$$\begin{aligned} r_i(T) \quad = \quad & A_+ F_+(\psi, \hat{\boldsymbol{k}}, \hat{\boldsymbol{n}}_i)\Big[\cos\left(\omega t_i^e + \phi_0\right)\exp\Big(-\frac{(t_i^e)^2}{2\tau^2}\Big) \\ & -\cos\left(\omega t_i^p + \phi_0\right)\exp\Big(-\frac{(t_i^p)^2}{2\tau^2}\Big)\Big] + \\ & A_\times F_\times(\psi, \hat{\boldsymbol{k}}, \hat{\boldsymbol{n}}_i)\Big[\sin\left(\omega t_i^e + \phi_0\right)\exp\Big(-\frac{(t_i^e)^2}{2\tau^2}\Big) \\ & -\sin\left(\omega t_i^p + \phi_0\right)\exp\Big(-\frac{(t_i^p)^2}{2\tau^2}\Big)\Big], \end{aligned} \tag{6}$$

where $A_+ = A(1+\cos^2\iota)/2$ and $A_\times = A\cos\iota$ for an amplitude A and source inclination angle ι, τ is the Gaussian width, ω is the angular frequency, ϕ_0 is the phase at the midpoint of the burst, and the definitions of the antenna patterns $F_{+/\times}$ are described in Appendix A. The times are defined so that the *PT* is described by the terms containing $t^p = T - t_i$, where T is the pulsar proper time at the solar system barycentre and t_i is time at the observed midpoint of the burst in the *PT* (as seen for a particular pulsar), and therefore the *ET* time is described by the terms containing $t^e = T - t_i + (1 + \hat{\boldsymbol{k}}\cdot\hat{\boldsymbol{n}}_i)d_i/c$. This could be expanded to a physical source model such as the parabolic encounter of two supermassive black holes used in Finn & Lommen (2010) (which is qualitatively similar to a sine-Gaussian), or a more generic burst model as employed in ground-based detector searches.

3.2 Event rates for detection

It is useful to try and compare the source event rates that would be required to detect a signal in the *ET*s of all pulsars in the IPTA to that which would be required to detect a signal in the *PT*s of pairs of pulsars in the IPTA. We have made some general estimates of this for the sine-Gaussian signal described in Section 3.1, with fixed parameters (following the definition in Equation 6): $A = 500$ ns, $\omega = 2\pi \times 4\,\mathrm{yr}^{-1}$, $\psi = 0$ rads, $\phi_0 = 2.0$ rads, $\tau = 100$ days and with the burst centred on the midpoint of the observations.

We define the signal-to-noise ratio to a given signal, r, for a set of N pulsars as

$$\rho = \left(\sum_{i=1}^{N}\sum_{j=1}^{n_i}\frac{r_j^2}{\sigma_i^2}\right)^{1/2}, \tag{7}$$

where n_i is the number of residual data points, and σ_i is the noise standard deviation, for the i^{th} pulsar (working in the time domain).

3.2.1 Search sensitivity and range

Using Equation 7 we have calculated the signal-to-noise ratio for the sine-Gaussian source defined above at each point in the sky for the IPTA pulsars. Figure 6(a) shows the signal-to-noise ratio that this source (if optimally oriented with $\cos\iota = \pm 1$) could be observed at if located across the sky and seen in the *ET*s for the entire IPTA. The flower-like patterns in the response across the sky come

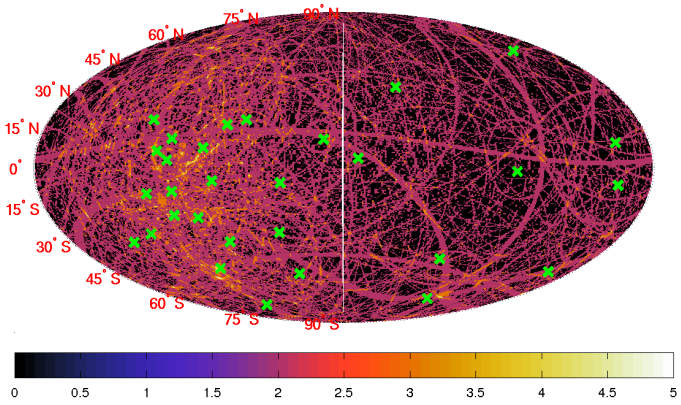

(a)

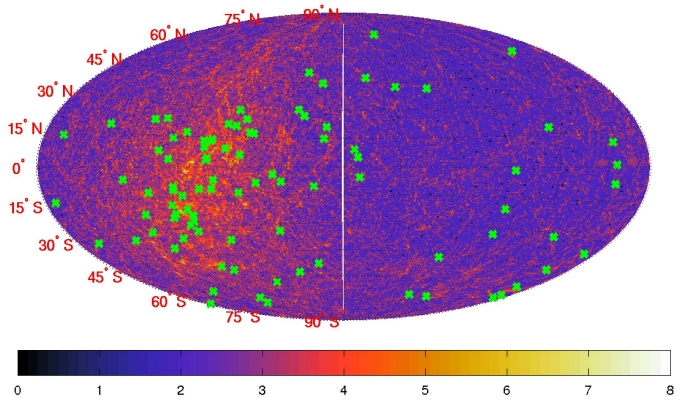

(b)

Figure 5. (a) The number of pulsars with *PT*s separated by less that 10 years for given source sky locations using the ITPA. (b) The number of pulsars with *PT*s separated by less that 10 years for given source sky locations using a fake PTA of 91 pulsars.

from the antenna patterns of pairs of pulsars as seen in Figures A1 and A2. The range of signal-to-noise ratios for this particular source over the sky was between 40.7 and 14.8, whereas if the the worst case source orientation were chosen ($\cos\iota = 0$) then the signal-to-noise ratio was between 10.0 and 2.5.

Figure 6(b) shows the *maximum* signal-to-noise ratio that this source (if optimally oriented with $\cos\iota = \pm 1$) could be observed at if located across the sky and seen in the *PT*s of pairs (or multiples when applicable) of IPTA pulsars. We define regions of the sky with no pulsar pairs *PT*s separated by less than 10 years as having zero signal-to-noise i.e. we assume that we could not see, or would ignore as potential noise, a *PT* signal only observed in one pulsar. In this case what we mean by *maximum* is that for locations for which multiple pulsar pairs could contain signals we have taken the signal-to-noise ratio of the loudest pair. Over the sky area that could be observed ($\sim$ 67 per cent of the sky) the range of signal-to-noise ratios for the *maximum* and optimally oriented case was between 19.4 and 0.4, whereas for the worst case orientation (and with the quietest pulsar pair chosen) the ranges was between 4.6 and 7×10^{-4} (see Figure 6(c)).

The ratio of signal-to-noise ratios between an *ET* search (using all 30 pulsars) and a *PT* search (using only a pair of pulsars for each sky position) agree well with the simple calculation of $\sqrt{30/2} \approx 4$.

From Figure 6 we can calculate a sky-averaged signal to noise ratios, $\langle\rho\rangle$, for a detectable source. For the example case above of using the *ET*s for the search and an optimally oriented source $\langle\rho\rangle = 26.7$. We know that the signal amplitude that led to this was $A = 500\,\mathrm{ns}$, so assuming that we want a source to have $\langle\rho\rangle \geqslant 10$ for detection we can scale the signal amplitude appropriately giving an effective sky averaged amplitude required for detection of

$$\langle A\rangle \geqslant 500 \times \left(\frac{10}{26.7}\right)\,\mathrm{ns} = 187\,\mathrm{ns}. \tag{8}$$

To set a scale (which will effect the absolute values of our event rates estimated below, but will not effect the relative ratios between them), we will say that a source at a distance of 1 Gpc produces an amplitude in the pulsar residuals of 100 ns. The observed amplitude is directly proportional to the source distance D, so for detection we require that

$$\left(\frac{D}{1\,\mathrm{Gpc}}\right) \leqslant \left(\frac{100\,\mathrm{ns}}{\langle A\rangle\,\mathrm{ns}}\right), \tag{9}$$

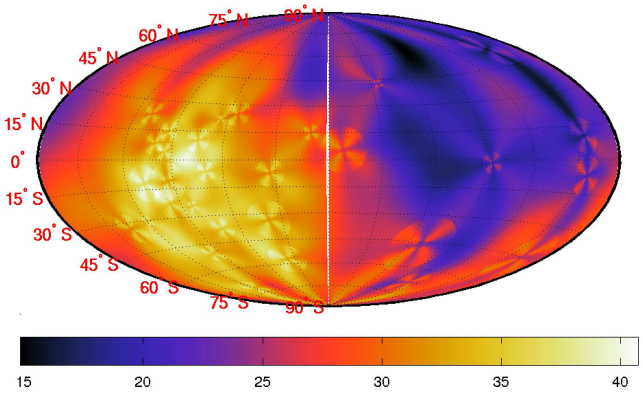

(a)

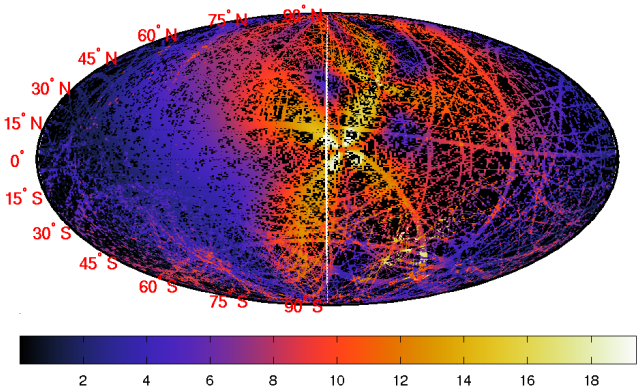

(b)

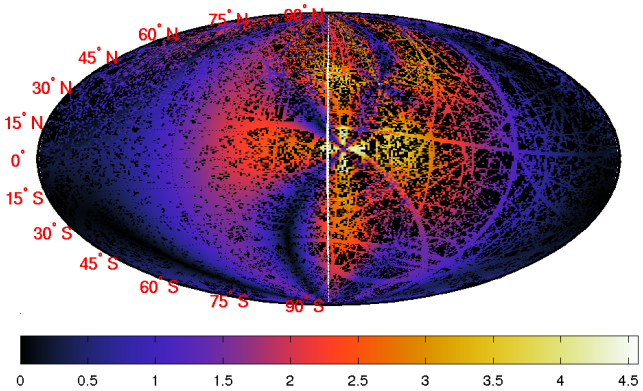

(c)

Figure 6. Hammer projection sky maps giving the signal-to-noise ratios for a source located at different sky locations for the IPTA observations with: (a) the signal appearing in the *ET*s of all pulsars for an optimally oriented source; (b) the signal appearing in the *PT*s for pairs (or multiples) of pulsars for an optimally oriented source and using the loudest pair for a given sky location; and, (c) the signal appearing in the *PT*s for pairs (or multiples) of pulsars for the worst source orientation and using the quietest pair for a given sky location.

or more generically

$$\left(\frac{D}{1\,\mathrm{Gpc}}\right) \leqslant \left(\frac{100\,\mathrm{ns}}{A\,\mathrm{ns}}\right)\left(\frac{\langle\rho\rangle_A}{\langle\rho\rangle_{\mathrm{thresh}}}\right), \quad (10)$$

where A is the observed signal amplitude that gives a sky-averaged signal-to-noise ratio of $\langle\rho\rangle_A$, and $\langle\rho\rangle_{\mathrm{thresh}}$ is the signal-to-noise ratio threshold for detection (so given the case in Equation 8 $A = 500\,\mathrm{ns}$, $\langle\rho\rangle_A = 26.7$ and $\langle\rho\rangle_{\mathrm{thresh}} = 10$). This gives us a sky-averaged range, or horizon distance (similar to that used as a figure of merit for compact binary coalescences in ground-based gravitational wave detectors e.g. Abbott et al. 2005), as a function of the observed amplitude.

From Figure 6 we can calculate that for the *ET* search the best and worst case sky-averaged signal-to-noise ratios, $\langle\rho\rangle$ are 26.7 and 6.4 respectively, giving horizon distances of 0.53 and 0.13 Gpc. For the *PT* search the best and worst case sky-averaged signal-to-noise ratios, $\langle\rho\rangle$ are 6.6 and 1.3 respectively, giving horizon distances of 0.13 and 0.03 Gpc.

3.2.2 *Effective observation times*

For the *ET* search each pulsar observes the whole sky, so the effective total observation time, T_{tot}, is just the span of the residual observations $T_{\mathrm{tot},ET} = T_{\mathrm{res}}$, but for the *PT* search the calculation is more complex. For a pulsar pair the overlapping observation time that could contain a signal (assuming that the signal width is small compared to the data span) will be $T_{\mathrm{res}} - \Delta t$, where Δt is the maximum delay between *PT*s. Also, whereas in the *ET* search each pulsar observes the whole sky, in the *PT* search each pulsar pair will only have a fractional sky coverage that gives *PT*s within Δt (the ring on the sky in Figure 2). So, for a particular pulsar pair the observation time factored by the sky coverage will be

$$T_{\mathrm{obs},i} = (T_{\mathrm{res}} - \Delta t) \times f_i, \quad (11)$$

where f_i is the fractional sky coverage for that pair. The effective total observation time will therefore be $T_{\mathrm{tot},PT} = \sum_i^N T_{\mathrm{obs},i}$, where N is the number of pulsar pairs. As we are assuming T_{res} and Δt are the same for all pulsar pairs this becomes

$$T_{\mathrm{tot},PT} = (T_{\mathrm{res}} - \Delta t) \times \sum_i^N f_i. \quad (12)$$

So, for the *PT* search the lack of sky coverage for individual pulsar pairs can be compensated for by the effective increase in the temporal coverage i.e. each pulsar pair sees a different time epoch, but can only see that epoch for a small portion of the sky.

For $T_{\mathrm{res}} = 20$ years and $\Delta t = 10$ years we find that for all IPTA pulsar pairs the sum of their fractional sky coverage is $\sum_{i=1}^{435} f_i = 1.15$. This means that $T_{\mathrm{tot},PT} = 20$ years and $T_{\mathrm{tot},ET} = 11.5$, which are comparable. In the next section we discuss what this indicates in terms of event rates.

3.2.3 *Source event rates*

If we assume that the rate of events that would produce an observed signal amplitude of 100 ns if at a distance of 1 Gpc, R (per unit volume per unit time), is the same throughout the Universe we can approximate the observed number of events, O, as

$$O = R \times \frac{4}{3}\pi D^3 \times T_{\mathrm{tot}}. \quad (13)$$

Using the horizon distances calculated above we can use Equation 13 to calculate the rate of these events (i.e. the rate of sources that would produce a 100 ns amplitude signal if at 1 Gpc) against total observation time if we want to be able to observe one signal. This is shown in Figure 7 along with lines corresponding to the effective observation times of an *ET* search and a *PT* search. We find that for the *ET* search, with an effective observation time of $T_{\mathrm{tot}} = 20$ years, source event rates of $\sim 0.08\,\mathrm{Gpc}^{-3}\,\mathrm{yr}^{-1}$ and $\sim 5.5\,\mathrm{Gpc}^{-3}\,\mathrm{yr}^{-1}$ would be required to observe one event assuming all sources are either in the best case or worst case orientations respectively. For a search using the *PT*s, with an effective observation time of $T_{\mathrm{tot}} = 11.5$ years, source event rates of $\sim 9.6\,\mathrm{Gpc}^{-3}\,\mathrm{yr}^{-1}$ and $\sim 790\,\mathrm{Gpc}^{-3}\,\mathrm{yr}^{-1}$ would be required to observe one event with the best case and worst case orientations respectively. This suggests that many sources should be observed in an *ET* search if you were to observed one in the *PT* search, or conversely if you observed one event in an *ET* search you would expect it to be very unlikely that a *PT* search would also produce an observed signal.

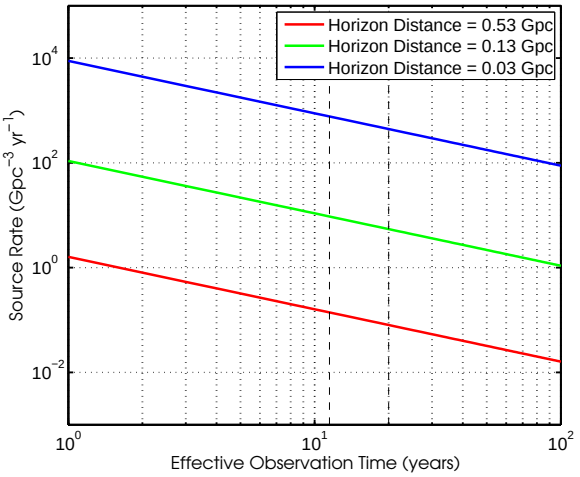

Figure 7. The source event rate as a function of effective observation times required to observed one event for a variety of detector horizon distances. The vertical dashed lines show the effective observation times for a search using the *PT*s (left) and *ET*s (right) with the IPTA pulsars.

3.2.4 *An expanded array*

Using the example of the IPTA above we can scale values to see how *ET* searches and *PT* searches would compare for a larger array of N pulsars given a fixed source event rate R. For an *ET* search, given that the observation time is fixed, the number of events that will be observed is dependent on the observing volume, which itself depends in the horizon distance, which corresponds to the observed sky-averaged signal-to-noise ratio. The signal-to-noise ratio increases with the square root of the number of pulsars in the array, so overall the observed number of events becomes

$$O_{ET} = R \times \frac{4}{3}\pi \left(D_{ET,\mathrm{IPTA}}\left(\frac{N}{30}\right)^{1/2}\right)^3 \times T_{\mathrm{tot},ET} \quad (14)$$

where $D_{ET,\mathrm{IPTA}}$ and $T_{ET,\mathrm{tot}}$ are the horizon distance and effective observation times for the *ET* search using the IPTA above. For the *PT* search the signal-to-noise ratio, and hence horizon distance and observed volume, is fixed (assuming that we still only use pairs of pulsars, rather than more), but the effective total observation time changes. If each pulsar pair sees on average a fraction $\bar{f}$ of the sky,

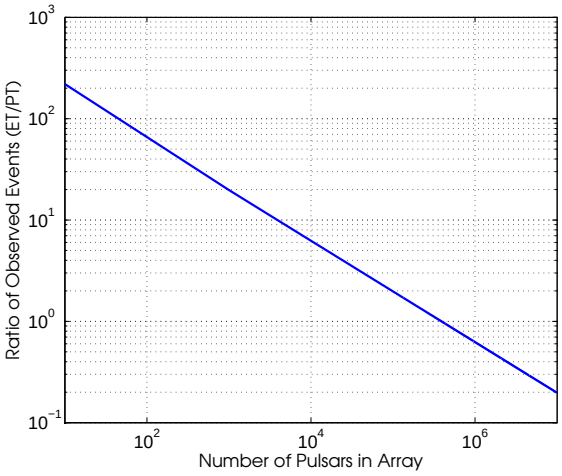

Figure 8. The ratio of the number of events observable in an *ET* search compared to that observable in an *PT* search as a function of the number of pulsars in a PTA.

and the number of pulsar pairs given N pulsars is $N(N-1)/2$, then the effective observation time is proportional to $\bar{f}N(N-1)/2$, and the observed number of events becomes

$$O_{PT} = R \times \frac{4}{3}\pi D^3_{PT,\mathrm{IPTA}} \times T_{PT}\bar{f}N(N-1)/2, \qquad (15)$$

where $D_{PT,\mathrm{IPTA}}$ is the horizon distance for the *PT* search using the IPTA above and $T_{PT} = T_{\mathrm{res}} - \Delta t = 10$ years as above. It can be seen that Equation 14 scales as $N^{3/2}$ whereas Equation 15 scales as N^2, so for a fixed rate (provided the sources and event rates are isotropic within the horizon distance) and a large enough array of pulsars the number of events observable in a *PT* search should overtake that observable in an *ET* search, i.e. the total effective observation time available will compensate for the smaller range.

Using the numbers for the IPTA (i.e. assuming a maximum delay between *PT*s of 10 years) we see that the average sky fraction observed by a pulsar pair is $\bar{f} = 1.15/435 = 0.0026$. Using the horizon distances for the best case orientation for the *ET* and *PT* searches Figure 8 shows the ratio of the observable number of events in an *ET* search to a *PT* search as a function of the number of pulsars in an array. We see that to achieve equality in the number of events observed would require an array of $\sim 400\,000$ pulsars. This is greater than the total expected number of active pulsars in the Galaxy (Lorimer 2008), so is not achievable.

4 SUMMARY

In searches for stochastic or burst sources of gravitational waves in PTA data the delayed *PT* is often ignored as it will generally be incoherent between residuals from different pulsars. We have looked at whether extra value could be gained when looking for short duration burst sources by looking for coherent signals in *PT*s from pairs, or more, of pulsars for specific source sky locations. In the era of the Low Frequency Array (LOFAR)/SKA it could be possible to observe a few thousand millisecond pulsars (Smits et al. 2009), with around 100 of the best timed of these being usable as "arms" in a PTA (Kramer 2012). However, our studies have mainly focused on the possibilities using the IPTA, containing 30 pulsars.

We have shown that for a PTA timing array there can be significant areas of the sky containing a source for which the *PT*s of a signal can appear separated by relatively short times in pairs of pulsar residuals. In particular for the IPTA we find that this is the case for 67 per cent of the sky given maximum delays between *PT*s in two pulsars of 10 years. To accurately know which sky locations this is valid for would require precise (sub one per cent) knowledge of the PTA pulsar distances. This may be possible in the future with the SKA, but otherwise any search would have to take into account the distance uncertainties. For arrays of more pulsars the sky coverage becomes greater, e.g. for 90 pulsars almost the whole sky is covered, and there also become more source sky locations that give *PT*s observable in more than two pulsars.

We have also compared the relative sky-averaged sensitivities of a search using the *ET*s, which are coherent between all pulsars in the PTA, with that of a search that uses the *PT*s in pairs of pulsars. Considering an optimally oriented source, and using the pulsar pair with the largest antenna pattern for a given sky location, we find that the *ET* search is on average about four times more sensitive. For the worst case source orientation, and using the pulsar pair with the smallest antenna pattern we find that the *ET* search is on average five times more sensitive. These are very comparable with what might be expected given that the *ET* search uses 30 pulsars, whereas the *PT* search is generally just using pairs of pulsar i.e. $\sqrt{30/2} \approx 4$. An *ET* search would require a signal to occur within the observation window of the residuals, whereas each *PT* search would be looking back in time covering some time window dependent of the delay between pulsar terms. However, the *ET* search would cover the whole sky whereas the searches for *PT*s in pairs of pulsars would only cover small parts of the sky. For residual observations covering 20 years and maximum delays between *PT*s of less than 10 years we have found that a *PT* search would have an effective observation time of 11.5 years taking into account the limited sky coverage for each pulsar pair. We have converted these sensitivities to horizon distances for a putative source, and along with the effective observation times, used them to estimate the event rates required to observe one event in the *ET*s and *PT*s of a simulated IPTA with 20 years of residuals. We have found that event rates for comparable sources show that you would have approximately two orders of magnitude higher chance of observing a signal in the *ET*s than the *PT*s for an *all-sky* search. However, this does not mean that *PT* searches are pointless. They could be complementary to *ET* searches in helping add more observation time to specific targets in the sky like large galaxy clusters. We have also assumed that all pulsar residuals have equivalent noise levels, but it could be that the least noisy pulsars could dominate the sensitivity and improve the comparisons.

For arrays of larger numbers of pulsars we have seen that the scaling of the total effective observation time for a *PT* search rises faster than the search volume of the *ET* search. However, unfortunately the potential observable number of events in a *PT* search does not rise above that for an *ET* search until $\sim 400\,000$ pulsars are in the array. Unfortunately such a large array is a completely unachievable goal. However, in larger arrays much more of the sky would be covered be cases when more that two pulsars have *PT*s separated by less than 10 years, so this would potentially bring that ratio down to a more hopeful level.

In future work we plan to: investigate a more realistic timing array with more physical pulsar residuals; test and characterise a search routine; and, if possible, apply it to real data, or future IPTA

mock data challenges[3]. These studies will show whether the results here are more pessimistic than necessary.

ACKNOWLEDGEMENTS

This work has been funded under a UK Science and Technology Facilities Council rolling grant. I would like to thank Andrea Lommen and Graham Woan for discussions that lead to this work and for comments on drafts of this paper. I thank the referees for many valuable comments on the paper and in particular for the suggestion to look at comparisons between "Earth term" and "pulsar term" searches.

REFERENCES

Abbott B. et al., 2005, Phys. Rev. D, 72, 082001
Abbott B. P. et al., 2009, Phys. Rev. D, 80, 102001
Anholm M., Ballmer S., Creighton J. D. E., Price L. R., Siemens X., 2009, Phys. Rev. D, 79, 084030
Babak S. et al., 2010, Classical and Quantum Gravity, 27, 084009
Babak S., Sesana A., 2012, Phys. Rev. D, 85, 044034
Binétruy P., Bohé A., Hertog T., Steer D. A., 2009, Phys. Rev. D, 80, 123510
Clark J., Heng I. S., Pitkin M., Woan G., 2007, Phys. Rev. D, 76, 043003
Corbin V., Cornish N. J., 2010, arXiv:1008.1782
Cordes J. M., Jenet F. A., 2012, ApJ, 752, 54
Davis M. M., Taylor J. H., Weisberg J. M., Backer D. C., 1985, Nature, 315, 547
Demorest P. B. et al., 2012, arXiv:1201.6641
Deng X., Finn L. S., 2011, MNRAS, 414, 50
Detweiler S., 1979, ApJ, 234, 1100
Ellis J., Siemens X., Creighton J., 2012, arXiv:1204.4218
Ellis J. A., Jenet F. A., McLaughlin M. A., 2012, ApJ, 753, 96
Estabrook F. B., Wahlquist H. D., 1975, General Relativity and Gravitation, 6, 439
Ferdman R. D. et al., 2010, Classical and Quantum Gravity, 27, 084014
Finn L. S., 2009, Phys. Rev. D, 79, 022002
Finn L. S., Lommen A. N., 2010, ApJ, 718, 1400
Foster R. S., Backer D. C., 1990, ApJ, 361, 300
Hellings R. W., Downs G. S., 1983, ApJ, 265, L39
Hobbs G. et al., 2010, Classical and Quantum Gravity, 27, 084013
Jaffe A. H., Backer D. C., 2003, ApJ, 583, 616
Jenet F. et al., 2009, arXiv:0909.1058
Jenet F. A., Creighton T., Lommen A., 2005, ApJ, 627, L125
Jenet F. A., Hobbs G. B., Lee K. J., Manchester R. N., 2005, ApJ, 625, L123
Jenet F. A. et al., 2006, ApJ, 653, 1571
Jenet F. A., Lommen A., Larson S. L., Wen L., 2004, ApJ, 606, 799
Kaspi V. M., Taylor J. H., Ryba M. F., 1994, ApJ, 428, 713
Key J. S., Cornish N. J., 2009, Phys. Rev. D, 79, 043014
Klimenko S., Yakushin I., Mercer A., Mitselmakher G., 2008, Classical and Quantum Gravity, 25, 114029
Kramer M., 2012, in IAU Symposium, Vol. 285, New Horizons in Time-Domain Astronomy, Griffin R. E. M., Hanisch R. J., Seaman R., eds., Cambridge University Press, pp. 147–152
Leblond L., Shlaer B., Siemens X., 2009, Phys. Rev. D, 79, 123519
Lee K. J., Wex N., Kramer M., Stappers B. W., Bassa C. G., Janssen G. H., Karuppusamy R., Smits R., 2011, MNRAS, 414, 3251
Lommen A. N., 2001, PhD thesis, University of California, Berkeley
Lommen A. N., 2012, Journal of Physics Conference Series, 363, 012029
Lommen A. N., Backer D. C., 2001, ApJ, 562, 297
Lorimer D. R., 2008, Living Reviews in Relativity, 11, 8, `http://www.livingreviews.org/lrr-2008-8`
Manchester R. N., Hobbs G. B., Teoh A., Hobbs M., 2005, AJ, 129, 1993
McHugh M. P., Zalamansky G., Vernotte F., Lantz E., 1996, Phys. Rev. D, 54, 5993
Mingarelli C. M. F., Grover K., Sidery T., Smith R. J. E., Vecchio A., 2012, arXiv:1207.5645
Pshirkov M. S., Baskaran D., Postnov K. A., 2010, MNRAS, 402, 417
Rawley L. A., Taylor J. H., Davis M. M., Allan D. W., 1987, Science, 238, 761
Romani R. W., Taylor J. H., 1983, ApJ, 265, L35
Sazhin M. V., 1978, Soviet Ast., 22, 36
Searle A. C., Sutton P. J., Tinto M., 2009, Classical and Quantum Gravity, 26, 155017
Sesana A., Vecchio A., Volonteri M., 2009, MNRAS, 394, 2255
Smits R., Kramer M., Stappers B., Lorimer D. R., Cordes J., Faulkner A., 2009, A&A, 493, 1161
Smits R., Tingay S. J., Wex N., Kramer M., Stappers B., 2011, A&A, 528, A108
Stinebring D. R., Ryba M. F., Taylor J. H., Romani R. W., 1990, Phys. Rev. Lett., 65, 285
Sutton P. J. et al., 2010, New Journal of Physics, 12, 053034
van Haasteren R., Levin Y., 2010, MNRAS, 401, 2372
van Haasteren R. et al., 2011, MNRAS, 414, 3117
van Haasteren R., Levin Y., McDonald P., Lu T., 2009, MNRAS, 395, 1005
Verbiest J. P. W. et al., 2010, Classical and Quantum Gravity, 27, 084015
Wyithe J. S. B., Loeb A., 2003, ApJ, 590, 691
Yardley D. R. B. et al., 2011, MNRAS, 414, 1777
Yardley D. R. B. et al., 2010, MNRAS, 407, 669

APPENDIX A: THE ANTENNA PATTERN

Given $\hat{\boldsymbol{k}}$ is a unit vector pointing along the wave propagation direction from the source to the Earth we can construct the following basis vectors representing the wave propagation frame,

$$\hat{\boldsymbol{k}} = (-\sin\theta_s\cos\phi_s, -\sin\theta_s\sin\phi_s, -\cos\theta_s), \quad \text{(A1)}$$

$$\hat{\boldsymbol{l}} = (\sin\phi_s, -\cos\phi_s, 0), \quad \text{(A2)}$$

$$\hat{\boldsymbol{m}} = (\cos\theta_s\cos\phi_s, \cos\theta_s\sin\phi_s, -\sin\theta_s), \quad \text{(A3)}$$

and define the unit vector from the Earth (or more correctly the solar system barycentre) to the pulsar $\hat{\boldsymbol{n}} = (\sin\theta_p\cos\phi_p, \sin\theta_p\sin\phi_p, \cos\theta_p)$, where $\phi_{s,p}$ give the right ascensions and $\theta_{s,p} = \pi/2 - \text{declination}$ for the source and pulsar respectively. From these the polarisation basis tensors can be de-

[3] `http://www.ipta4gw.org/`

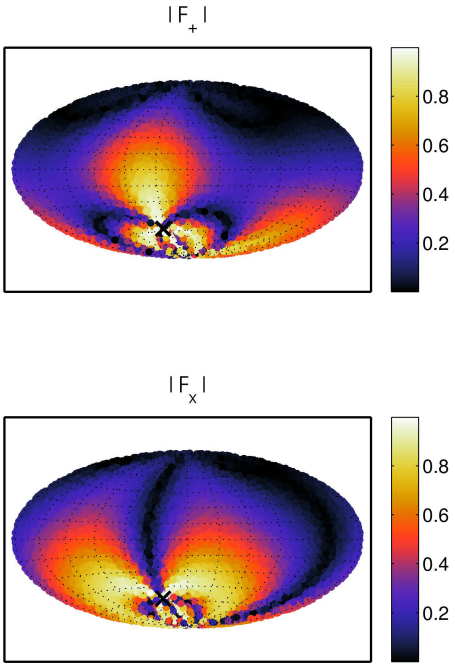

Figure A1. The absolute values of the 'plus' and 'cross' polarisation antenna pattern for pulsar J2129−5721 ($\alpha = 21^{\rm h}29^{\rm m}22\overset{\rm s}{.}7$, $\delta = -57°21'14\overset{''}{.}1$) over the whole sky. The pulsar location is marked by the black cross.

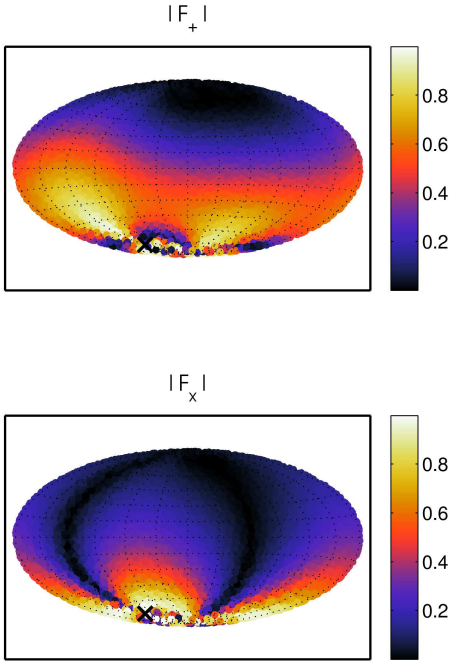

Figure A2. The absolute values of the 'plus' and 'cross' polarisation antenna pattern for pulsar J1603−7202 ($\alpha = 16^{\rm h}03^{\rm m}35\overset{\rm s}{.}6$, $\delta = -72°02'32\overset{''}{.}6$) over the whole sky. The pulsar location is marked by the black cross.

fined by

$$e^{ab}_{+} = l^a l^b - m^a m^b, \quad \text{(A4)}$$
$$e^{ab}_{\times} = l^a m^b + m^a l^b, \quad \text{(A5)}$$

and, with the inclusion of the polarisation angle ψ, by

$$e^{ab}_{+} = \cos(2\psi) e^{ab}_{+} + \sin(2\psi) e^{ab}_{\times}, \quad \text{(A6)}$$
$$e^{ab}_{\times} = -\sin(2\psi) e^{ab}_{+} + \cos(2\psi) e^{ab}_{\times}. \quad \text{(A7)}$$

The 'plus' and 'cross' antenna patterns (e.g. see Anholm et al. 2009 or Finn & Lommen 2010) are therefore given by

$$F_{+/\times} = \frac{1}{2} e^{ab}_{+/\times} \frac{\hat{\boldsymbol{n}}_a \hat{\boldsymbol{n}}_b}{1 + \hat{\boldsymbol{k}} \cdot \hat{\boldsymbol{n}}}. \quad \text{(A8)}$$

Examples of these full sky antenna patterns for a couple of pulsars, with $\psi = 0$, are given in Figures A1 and A2.

As we are not in the long wavelength approximation regime pulsar timing residuals will consist of components from the *ET* and *PT*, such that

$$r(T) = (A_+(t^e) - A_+(t^p)) F_+(\psi, \hat{\boldsymbol{k}}, \hat{\boldsymbol{n}}) + (A_\times(t^e) - A_\times(t^p)) F_\times(\psi, \hat{\boldsymbol{k}}, \hat{\boldsymbol{n}}) \quad \text{(A9)}$$

where, as we are dealing with the *PT*s in this paper, we set the time of the *PT* as $t^p = T - t_i$, where T is the pulsar proper time at the solar system barycentre and t_i is time at the observed midpoint of the burst in the pulsar term (as seen for a particular pulsar), and therefore the *ET* time is $t^e = T - t_i + (1 + \hat{\boldsymbol{k}} \cdot \hat{\boldsymbol{n}}_i) d_i / c$.

When creating a coherent signal in two pulsars' residuals the signal model for the second pulsar will have to be shifted by $\Delta t_{ij} = (1 + \hat{\boldsymbol{k}} \cdot \hat{\boldsymbol{n}}_i) d_i / c - (1 + \hat{\boldsymbol{k}} \cdot \hat{\boldsymbol{n}}_j) d_j / c$ with respect to the first pulsar i.e. if we have $r_1(T)$ then to coherently combine it with another dataset that would have to have $r_2(T + \Delta t_{12})$, with $t_i = t_1$ for both models.